

Observation of $B^0 \rightarrow D_s^+ \pi^-$

K. Abe,¹⁰ K. Abe,⁴⁶ N. Abe,⁴⁹ I. Adachi,¹⁰ H. Aihara,⁴⁸ M. Akatsu,²⁴ Y. Asano,⁵³
T. Aso,⁵² V. Aulchenko,² T. Aushev,¹⁴ T. Aziz,⁴⁴ S. Bahinipati,⁶ A. M. Bakich,⁴³
Y. Ban,³⁶ M. Barbero,⁹ A. Bay,²⁰ I. Bedny,² U. Bitenc,¹⁵ I. Bizjak,¹⁵ S. Blyth,²⁹
A. Bondar,² A. Bozek,³⁰ M. Bračko,^{22, 15} J. Brodzicka,³⁰ T. E. Browder,⁹ M.-C. Chang,²⁹
P. Chang,²⁹ Y. Chao,²⁹ A. Chen,²⁶ K.-F. Chen,²⁹ W. T. Chen,²⁶ B. G. Cheon,⁴
R. Chistov,¹⁴ S.-K. Choi,⁸ Y. Choi,⁴² Y. K. Choi,⁴² A. Chuvikov,³⁷ S. Cole,⁴³
M. Danilov,¹⁴ M. Dash,⁵⁵ L. Y. Dong,¹² R. Dowd,²³ J. Dragic,²³ A. Drutskoy,⁶
S. Eidelman,² Y. Enari,²⁴ D. Epifanov,² C. W. Everton,²³ F. Fang,⁹ S. Fratina,¹⁵
H. Fujii,¹⁰ N. Gabyshev,² A. Garmash,³⁷ T. Gershon,¹⁰ A. Go,²⁶ G. Gokhroo,⁴⁴
B. Golob,^{21, 15} M. Grosse Perdekamp,³⁸ H. Guler,⁹ J. Haba,¹⁰ F. Handa,⁴⁷ K. Hara,¹⁰
T. Hara,³⁴ N. C. Hastings,¹⁰ K. Hasuko,³⁸ K. Hayasaka,²⁴ H. Hayashii,²⁵ M. Hazumi,¹⁰
E. M. Heenan,²³ I. Higuchi,⁴⁷ T. Higuchi,¹⁰ L. Hinz,²⁰ T. Hojo,³⁴ T. Hokuue,²⁴
Y. Hoshi,⁴⁶ K. Hoshina,⁵¹ S. Hou,²⁶ W.-S. Hou,²⁹ Y. B. Hsiung,²⁹ H.-C. Huang,²⁹
T. Igaki,²⁴ Y. Igarashi,¹⁰ T. Iijima,²⁴ A. Imoto,²⁵ K. Inami,²⁴ A. Ishikawa,¹⁰ H. Ishino,⁴⁹
K. Itoh,⁴⁸ R. Itoh,¹⁰ M. Iwamoto,³ M. Iwasaki,⁴⁸ Y. Iwasaki,¹⁰ R. Kagan,¹⁴ H. Kakuno,⁴⁸
J. H. Kang,⁵⁶ J. S. Kang,¹⁷ P. Kapusta,³⁰ S. U. Kataoka,²⁵ N. Katayama,¹⁰ H. Kawai,³
H. Kawai,⁴⁸ Y. Kawakami,²⁴ N. Kawamura,¹ T. Kawasaki,³² N. Kent,⁹ H. R. Khan,⁴⁹
A. Kibayashi,⁴⁹ H. Kichimi,¹⁰ H. J. Kim,¹⁹ H. O. Kim,⁴² Hyunwoo Kim,¹⁷ J. H. Kim,⁴²
S. K. Kim,⁴¹ T. H. Kim,⁵⁶ K. Kinoshita,⁶ P. Koppenburg,¹⁰ S. Korpar,^{22, 15} P. Krizan,^{21, 15}
P. Krokovny,² R. Kulasiri,⁶ C. C. Kuo,²⁶ H. Kurashiro,⁴⁹ E. Kurihara,³ A. Kusaka,⁴⁸
A. Kuzmin,² Y.-J. Kwon,⁵⁶ J. S. Lange,⁷ G. Leder,¹³ S. E. Lee,⁴¹ S. H. Lee,⁴¹
Y.-J. Lee,²⁹ T. Lesiak,³⁰ J. Li,⁴⁰ A. Limosani,²³ S.-W. Lin,²⁹ D. Liventsev,¹⁴
J. MacNaughton,¹³ G. Majumder,⁴⁴ F. Mandl,¹³ D. Marlow,³⁷ T. Matsuiishi,²⁴
H. Matsumoto,³² S. Matsumoto,⁵ T. Matsumoto,⁵⁰ A. Matyja,³⁰ Y. Mikami,⁴⁷
W. Mitaroff,¹³ K. Miyabayashi,²⁵ Y. Miyabayashi,²⁴ H. Miyake,³⁴ H. Miyata,³² R. Mizuk,¹⁴
D. Mohapatra,⁵⁵ G. R. Moloney,²³ G. F. Moorhead,²³ T. Mori,⁴⁹ A. Murakami,³⁹
T. Nagamine,⁴⁷ Y. Nagasaka,¹¹ T. Nakadaira,⁴⁸ I. Nakamura,¹⁰ E. Nakano,³³ M. Nakao,¹⁰
H. Nakazawa,¹⁰ Z. Natkaniec,³⁰ K. Neichi,⁴⁶ S. Nishida,¹⁰ O. Nitoh,⁵¹ S. Noguchi,²⁵
T. Nozaki,¹⁰ A. Ogawa,³⁸ S. Ogawa,⁴⁵ T. Ohshima,²⁴ T. Okabe,²⁴ S. Okuno,¹⁶
S. L. Olsen,⁹ Y. Onuki,³² W. Ostrowicz,³⁰ H. Ozaki,¹⁰ P. Pakhlov,¹⁴ H. Palka,³⁰
C. W. Park,⁴² H. Park,¹⁹ K. S. Park,⁴² N. Parslow,⁴³ L. S. Peak,⁴³ M. Pernicka,¹³
J.-P. Perroud,²⁰ M. Peters,⁹ L. E. Piilonen,⁵⁵ A. Poluektov,² F. J. Ronga,¹⁰ N. Root,²
M. Rozanska,³⁰ H. Sagawa,¹⁰ M. Saigo,⁴⁷ S. Saitoh,¹⁰ Y. Sakai,¹⁰ H. Sakamoto,¹⁸
T. R. Sarangi,¹⁰ M. Satapathy,⁵⁴ N. Sato,²⁴ O. Schneider,²⁰ J. Schümann,²⁹ C. Schwanda,¹³
A. J. Schwartz,⁶ T. Seki,⁵⁰ S. Semenov,¹⁴ K. Senyo,²⁴ Y. Settai,⁵ R. Seuster,⁹
M. E. Sevier,²³ T. Shibata,³² H. Shibuya,⁴⁵ B. Shwartz,² V. Sidorov,² V. Siegle,³⁸
J. B. Singh,³⁵ A. Somov,⁶ N. Soni,³⁵ R. Stamen,¹⁰ S. Stanič,^{53, *} M. Starič,¹⁵ A. Sugi,²⁴
A. Sugiyama,³⁹ K. Sumisawa,³⁴ T. Sumiyoshi,⁵⁰ S. Suzuki,³⁹ S. Y. Suzuki,¹⁰ O. Tajima,¹⁰
F. Takasaki,¹⁰ K. Tamai,¹⁰ N. Tamura,³² K. Tanabe,⁴⁸ M. Tanaka,¹⁰ G. N. Taylor,²³
Y. Teramoto,³³ X. C. Tian,³⁶ S. Tokuda,²⁴ S. N. Tovey,²³ K. Trabelsi,⁹ T. Tsuboyama,¹⁰
T. Tsukamoto,¹⁰ K. Uchida,⁹ S. Uehara,¹⁰ T. Uglov,¹⁴ K. Ueno,²⁹ Y. Unno,³ S. Uno,¹⁰
Y. Ushiroda,¹⁰ G. Varner,⁹ K. E. Varvell,⁴³ S. Villa,²⁰ C. C. Wang,²⁹ C. H. Wang,²⁸

J. G. Wang,⁵⁵ M.-Z. Wang,²⁹ M. Watanabe,³² Y. Watanabe,⁴⁹ L. Widhalm,¹³
 Q. L. Xie,¹² B. D. Yabsley,⁵⁵ A. Yamaguchi,⁴⁷ H. Yamamoto,⁴⁷ S. Yamamoto,⁵⁰
 T. Yamanaka,³⁴ Y. Yamashita,³¹ M. Yamauchi,¹⁰ Heyoung Yang,⁴¹ P. Yeh,²⁹ J. Ying,³⁶
 K. Yoshida,²⁴ Y. Yuan,¹² Y. Yusa,⁴⁷ H. Yuta,¹ S. L. Zang,¹² C. C. Zhang,¹² J. Zhang,¹⁰
 L. M. Zhang,⁴⁰ Z. P. Zhang,⁴⁰ V. Zhilich,² T. Ziegler,³⁷ D. Žontar,^{21,15} and D. Zürcher²⁰

(The Belle Collaboration)

¹*Aomori University, Aomori*

²*Budker Institute of Nuclear Physics, Novosibirsk*

³*Chiba University, Chiba*

⁴*Chonnam National University, Kwangju*

⁵*Chuo University, Tokyo*

⁶*University of Cincinnati, Cincinnati, Ohio 45221*

⁷*University of Frankfurt, Frankfurt*

⁸*Gyeongsang National University, Chinju*

⁹*University of Hawaii, Honolulu, Hawaii 96822*

¹⁰*High Energy Accelerator Research Organization (KEK), Tsukuba*

¹¹*Hiroshima Institute of Technology, Hiroshima*

¹²*Institute of High Energy Physics,
Chinese Academy of Sciences, Beijing*

¹³*Institute of High Energy Physics, Vienna*

¹⁴*Institute for Theoretical and Experimental Physics, Moscow*

¹⁵*J. Stefan Institute, Ljubljana*

¹⁶*Kanagawa University, Yokohama*

¹⁷*Korea University, Seoul*

¹⁸*Kyoto University, Kyoto*

¹⁹*Kyungpook National University, Taegu*

²⁰*Swiss Federal Institute of Technology of Lausanne, EPFL, Lausanne*

²¹*University of Ljubljana, Ljubljana*

²²*University of Maribor, Maribor*

²³*University of Melbourne, Victoria*

²⁴*Nagoya University, Nagoya*

²⁵*Nara Women's University, Nara*

²⁶*National Central University, Chung-li*

²⁷*National Kaohsiung Normal University, Kaohsiung*

²⁸*National United University, Miao Li*

²⁹*Department of Physics, National Taiwan University, Taipei*

³⁰*H. Niewodniczanski Institute of Nuclear Physics, Krakow*

³¹*Nihon Dental College, Niigata*

³²*Niigata University, Niigata*

³³*Osaka City University, Osaka*

³⁴*Osaka University, Osaka*

³⁵*Panjab University, Chandigarh*

³⁶*Peking University, Beijing*

³⁷*Princeton University, Princeton, New Jersey 08545*

³⁸*RIKEN BNL Research Center, Upton, New York 11973*

³⁹*Saga University, Saga*

- ⁴⁰*University of Science and Technology of China, Hefei*
⁴¹*Seoul National University, Seoul*
⁴²*Sungkyunkwan University, Suwon*
⁴³*University of Sydney, Sydney NSW*
⁴⁴*Tata Institute of Fundamental Research, Bombay*
⁴⁵*Toho University, Funabashi*
⁴⁶*Tohoku Gakuin University, Tagajo*
⁴⁷*Tohoku University, Sendai*
⁴⁸*Department of Physics, University of Tokyo, Tokyo*
⁴⁹*Tokyo Institute of Technology, Tokyo*
⁵⁰*Tokyo Metropolitan University, Tokyo*
⁵¹*Tokyo University of Agriculture and Technology, Tokyo*
⁵²*Toyama National College of Maritime Technology, Toyama*
⁵³*University of Tsukuba, Tsukuba*
⁵⁴*Utkal University, Bhubaneswer*
⁵⁵*Virginia Polytechnic Institute and State University, Blacksburg, Virginia 24061*
⁵⁶*Yonsei University, Seoul*

Abstract

We report the first observation of $B^0 \rightarrow D_s^+ \pi^-$ and an improved measurement of $\bar{B}^0 \rightarrow D_s^+ K^-$ based on 274×10^6 $B\bar{B}$ events collected with the Belle detector at KEKB. We measure the branching fractions $\mathcal{B}(\bar{B}^0 \rightarrow D_s^+ K^-) = (2.93 \pm 0.55 \pm 0.79) \times 10^{-5}$ and $\mathcal{B}(B^0 \rightarrow D_s^+ \pi^-) = (1.94 \pm 0.47 \pm 0.52) \times 10^{-5}$.

PACS numbers: 13.25.Hw, 14.40.Nd

The unitarity of the Cabbibo-Kobayashi-Maskawa (CKM) matrix [1] is a crucial component of the Standard Model, one that is currently being tested in multiple aspects through B meson decays at the B -factories. The decays $B^0 \rightarrow D_s^+ \pi^-$ are expected to proceed dominantly through a spectator process involving the $b \rightarrow u$ transition and are thus considered a promising mode for the precise determination of $|V_{ub}|$ [2]. The decay $\bar{B}^0 \rightarrow D_s^+ K^-$ is not directly accessible through a spectator process, requiring either final state interactions or a non-spectator W -exchange [3]. The decay $\bar{B}^0 \rightarrow D_s^+ K^-$ was observed by Belle [4] and confirmed by BaBar [5]. For $B^0 \rightarrow D_s^+ \pi^-$, both groups reported evidence [4, 5].

In this Letter we report improved measurements of $\bar{B}^0 \rightarrow D_s^+ K^-$ and $B^0 \rightarrow D_s^+ \pi^-$ decays with the Belle detector [6] at the KEKB asymmetric energy e^+e^- collider [7]. The results are based on a data sample, collected at the center-of-mass (CM) energy of the $\Upsilon(4S)$ resonance, which contains 274×10^6 produced $B\bar{B}$ pairs.

The Belle detector is a large-solid-angle magnetic spectrometer that consists of a silicon vertex detector (SVD), a 50-layer central drift chamber (CDC), an array of aerogel threshold Čerenkov counters (ACC), a barrel-like arrangement of time-of-flight scintillation counters (TOF), and an electromagnetic calorimeter (ECL) comprised of CsI(Tl) crystals located inside a superconducting solenoid coil that provides a 1.5 T magnetic field. An iron flux-return located outside of the coil is instrumented to detect K_L^0 mesons and to identify muons (KLM). The detector is described in detail elsewhere [6]. Two different inner detector configurations were used. For the first sample of 152 million $B\bar{B}$ pairs, a 2.0 cm radius beampipe and a 3-layer silicon vertex detector were used; for the latter 122 million $B\bar{B}$ pairs, a 1.5 cm radius beampipe, a 4-layer silicon detector and a small-cell inner drift chamber were used [8].

Charged tracks are selected with requirements based on the average hit residual and impact parameter relative to the interaction point (IP). We also require that the transverse momentum of the tracks be greater than 0.1 GeV/ c in order to reduce the low momentum combinatorial background. For charged particle identification (PID) the combined information from specific ionization in the central drift chamber (dE/dx), time-of-flight scintillation counters (TOF) and aerogel Čerenkov counters (ACC) is used. At large momenta (> 2.5 GeV/ c) only the ACC and dE/dx are used. Charged kaons are selected with PID criteria that have an efficiency of 88%, a pion misidentification probability of 8%, and negligible contamination from protons. The criteria for charged pions have an efficiency of 89% and a kaon misidentification probability of 9%. All tracks that are positively identified as electrons are rejected.

Neutral kaons are reconstructed via the decay $K_S^0 \rightarrow \pi^+ \pi^-$. The two-pion invariant mass is required to be within 6 MeV/ c^2 ($\sim 2.5\sigma$) of the nominal K^0 mass, and the displacement of the $\pi^+ \pi^-$ vertex from the IP in the transverse r - ϕ plane is required to be between 0.1 cm and 20 cm. The directions in the r - ϕ projection of the K_S^0 candidate's flight path and momentum are required to agree within 0.2 radians.

We reconstruct D_s^+ mesons in the channels $D_s^+ \rightarrow \phi \pi^+$, $\bar{K}^{*0} K^+$, and $K_S^0 K^+$ (inclusion of charge conjugate states is implicit throughout this report). ϕ (K^{*0}) mesons are formed from the $K^+ K^-$ ($K^+ \pi^-$) pairs with invariant mass within 10 MeV/ c^2 (50 MeV/ c^2) of the nominal ϕ (K^{*0}) mass. We select D_s^+ mesons in a wide (± 0.5 GeV/ c^2) window, for subsequent studies; the $M(D_s)$ signal region is defined to be within 12 MeV/ c^2 ($\sim 2.5\sigma$) of the nominal D_s^+ mass. D_s^+ candidates are combined with a charged kaon or pion to form a B meson. Candidate events are identified by their CM energy difference, $\Delta E = (\sum_i E_i) - E_b$, and the beam constrained mass, $M_{bc} = \sqrt{E_b^2 - (\sum_i \vec{p}_i)^2}$, where $E_b = \sqrt{s}/2$ is the beam

energy and \vec{p}_i and E_i are the momenta and energies of the decay products of the B meson in the CM frame. We select events with $M_{bc} > 5.2 \text{ GeV}/c^2$ and $|\Delta E| < 0.2 \text{ GeV}$ and define the B signal region to be $5.272 \text{ GeV}/c^2 < M_{bc} < 5.288 \text{ GeV}/c^2$ and $|\Delta E| < 0.03 \text{ GeV}$. The M_{bc} sideband is defined as $5.20 \text{ GeV}/c^2 < M_{bc} < 5.26 \text{ GeV}/c^2$. We use a Monte Carlo (MC) simulation to determine the efficiency [9].

To suppress the large combinatorial background that is dominated by the two-jet-like $e^+e^- \rightarrow q\bar{q}$ ($q = u, d, s$ and c quarks) continuum process, variables that characterize the event topology are used. We require $|\cos \theta_{\text{thr}}| < 0.80$, where θ_{thr} is the angle between the thrust axis of the B candidate and that of the rest of the event. This requirement eliminates 77% of the continuum background and retains 78% of the signal events. We also define a Fisher discriminant, \mathcal{F} , which is based on the production angle of the B candidate, the angle of the B candidate thrust axis with respect to the beam axis, and nine parameters that characterize the momentum flow in the event relative to the B candidate thrust axis in the CM frame [10]. We impose a requirement on \mathcal{F} that rejects 50% of the remaining continuum background and retains 92% of the signal.

We also consider possible backgrounds from $q\bar{q}$ events containing real D_s^+ mesons. These events peak in the $M(D_s)$ spectra but not in the ΔE and M_{bc} distributions. Thus it can be eliminated by fitting the ΔE distribution.

Other B decays, such as $\bar{B}^0 \rightarrow D^+\pi^-$, $D^+ \rightarrow K^-\pi^+\pi^+$, with one pion misidentified as a kaon, require particular attention because they have large branching fractions and can peak in the M_{bc} signal region. The reconstructed invariant mass spectra for these events overlap with the signal D_s^+ mass region, while their ΔE distribution is shifted by about $50 \text{ MeV}/c^2$. To suppress this background, we exclude event candidates that are consistent with the $D^+ \rightarrow K^-\pi^+\pi^+$ mass hypothesis within $15 \text{ MeV}/c^2$ ($\sim 3\sigma$) when the two same-sign particles are considered to be pions, independently of their PID information. For the $D_s^+ \rightarrow K_S^0 K^+$ mode there is a similar background from $\bar{B}^0 \rightarrow D^+\pi^-$, $D^+ \rightarrow K_S^0 \pi^+$. In this case we exclude candidates consistent within $20 \text{ MeV}/c^2$ ($\sim 3\sigma$) with the $D^+ \rightarrow K_S^0 \pi^+$ hypothesis.

Possible backgrounds from B decays via $b \rightarrow c$ transitions ($B \rightarrow D_s DX$) are also considered. The D_s mesons from these decays have a lower momentum and are kinematically separated from the signal. We analyzed a large MC sample of generic $B\bar{B}$ events and found no peaking backgrounds.

Another potential $B\bar{B}$ background is charmless $\bar{B}^0 \rightarrow K^- K^+ K^- \pi^+ (K_S^0 K^+ K^-)$. Such events peak in the ΔE and M_{bc} spectra, but not in the $M(D_s)$ distributions. They tend to be dominated by quasi-two-body decay channels such as $\phi \bar{K}^{*0}$ [11]. To reduce this background, we reject events with low ($< 2 \text{ GeV}/c^2$) two particle invariant masses: $M_{K^-\pi^+}$ and $M_{\phi K^-}$ for the $D_s^+ \rightarrow \phi \pi^+$ channel, $M_{K^+K^-}$ and $M_{\bar{K}^{*0}K^+}$ for $D_s^+ \rightarrow \bar{K}^{*0} K^+$, and $M_{K^+K^-}$ and $M_{K_S^0 K^-}$ for $D_s^+ \rightarrow K_S^0 K^+$. The remaining background from these sources, if any, is excluded by fitting the $M(D_s)$ distribution.

The scatter plots in ΔE and M_{bc} for the $\bar{B}^0 \rightarrow D_s^+ K^-$ and $B^0 \rightarrow D_s^+ \pi^-$ candidates in the $M(D_s)$ signal region are shown in Fig. 1; a significant enhancement in the B signal region is observed. Figure 2 shows the $M(D_s)$ spectra for selected $\bar{B}^0 \rightarrow D_s^+ K^-$ and $B^0 \rightarrow D_s^+ \pi^-$ candidates in the B signal region. In addition to clear signals at the D_s^+ mass in Fig. 2, we observe peaks at the D^+ mass, corresponding to $\bar{B}^0 \rightarrow D^+ \pi^-$ and $\bar{B}^0 \rightarrow D^+ K^-$, $D^+ \rightarrow \phi \pi^+$, $\bar{K}^{*0} K^+$, $K_S^0 K^+$.

Our studies have shown that the backgrounds may peak in the signal region of $M(D_s)$ or of ΔE (and M_{bc}) but not in both simultaneously. To extract our signal, we therefore

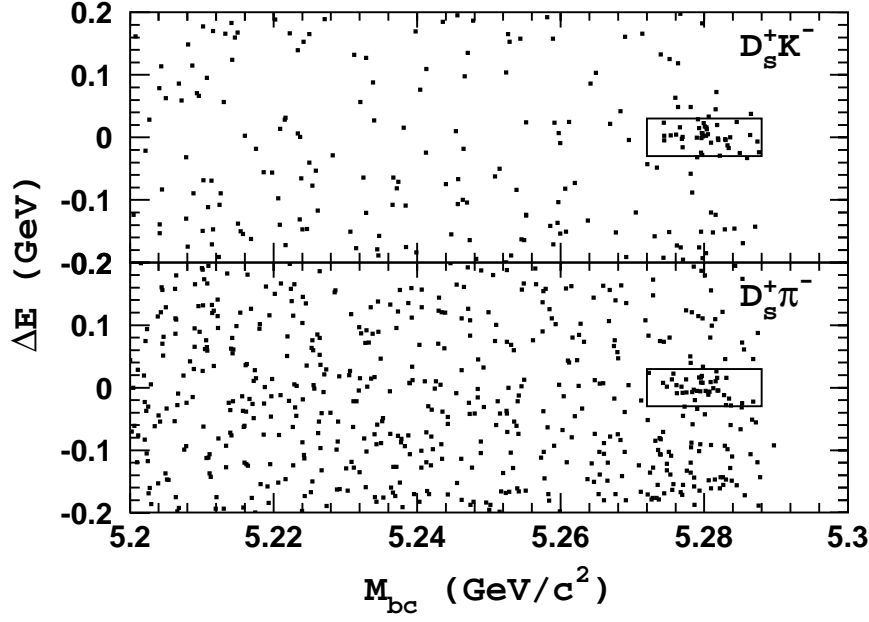


FIG. 1: ΔE versus M_{bc} scatter plot for the $\bar{B}^0 \rightarrow D_s^+ K^-$ (top) and $B^0 \rightarrow D_s^+ \pi^-$ (bottom) candidates in the $M(D_s)$ signal region. The points represent the experimental data and the boxes show the B meson signal region.

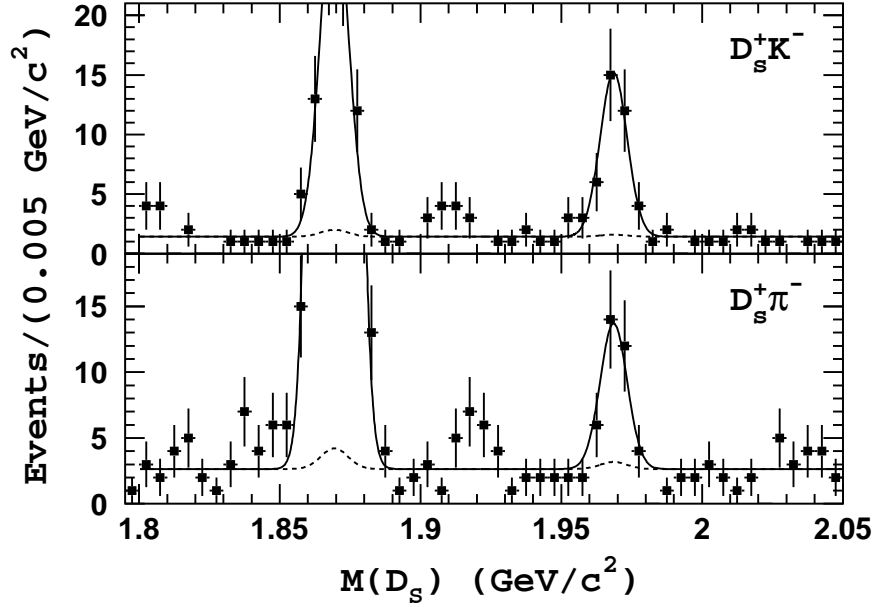


FIG. 2: $M(D_s)$ spectra for $\bar{B}^0 \rightarrow D_s^+ K^-$ (top) and $B^0 \rightarrow D_s^+ \pi^-$ (bottom) in the B signal region. The points with errors represent experimental data and the curves display the results of the simultaneous fit described in the text. The small feature near $1.92 \text{ GeV}/c^2$ arises due to favoured D^+ decays with pions misidentified as kaons.

TABLE I: Results on the signal yields and branching fractions. Decay channel, signal yield from two dimensional $M(D_s) - \Delta E$, one dimensional $M(D_s)$ and ΔE fits, detection efficiency branching fraction and statistical significance. The efficiencies include intermediate branching fractions.

Mode	$M(D_s) - \Delta E$	$M(D_s)$	ΔE	$\epsilon, 10^{-3}$	$\mathcal{B} (10^{-5})$	Significance
$\bar{B}^0 \rightarrow D_s^+ K^-, D_s^+ \rightarrow \phi \pi^+$	$18.2^{+5.0}_{-4.3}$	$18.2^{+4.7}_{-4.0}$	$18.1^{+4.9}_{-4.3}$	2.05	$3.25^{+0.89}_{-0.77} \pm 0.88$	6.2σ
$\bar{B}^0 \rightarrow D_s^+ K^-, D_s^+ \rightarrow \bar{K}^{*0} K^+$	$13.1^{+4.5}_{-3.8}$	$11.2^{+4.2}_{-3.6}$	$13.9^{+4.5}_{-3.9}$	1.49	$3.21^{+1.10}_{-0.93} \pm 0.87$	4.6σ
$\bar{B}^0 \rightarrow D_s^+ K^-, D_s^+ \rightarrow K_S^0 K^+$	$3.7^{+2.8}_{-2.2}$	$3.6^{+2.8}_{-2.1}$	$5.0^{+3.0}_{-2.3}$	0.86	$1.57^{+1.20}_{-0.94} \pm 0.42$	1.8σ
$\bar{B}^0 \rightarrow D_s^+ K^-, \text{simultaneous fit}$	$36.3^{+7.2}_{-6.6}$	$32.9^{+6.6}_{-5.9}$	$36.7^{+7.1}_{-6.4}$	4.29	$2.93 \pm 0.55 \pm 0.79$	7.9σ
$B^0 \rightarrow D_s^+ \pi^-, D_s^+ \rightarrow \phi \pi^+$	$12.7^{+4.4}_{-3.7}$	$14.4^{+4.2}_{-3.9}$	$11.7^{+4.3}_{-3.7}$	2.29	$2.03^{+0.70}_{-0.59} \pm 0.55$	4.5σ
$B^0 \rightarrow D_s^+ \pi^-, D_s^+ \rightarrow \bar{K}^{*0} K^+$	$7.0^{+4.3}_{-3.6}$	$5.3^{+3.9}_{-3.2}$	$9.3^{+4.5}_{-3.9}$	1.65	$1.54^{+0.95}_{-0.79} \pm 0.42$	2.1σ
$B^0 \rightarrow D_s^+ \pi^-, D_s^+ \rightarrow K_S^0 K^+$	$5.8^{+3.4}_{-2.7}$	$6.1^{+3.2}_{-2.6}$	$6.1^{+3.5}_{-2.8}$	0.89	$2.38^{+1.40}_{-1.12} \pm 0.64$	2.4σ
$B^0 \rightarrow D_s^+ \pi^-, \text{simultaneous fit}$	$25.7^{+6.5}_{-6.0}$	$26.3^{+6.4}_{-5.7}$	$27.3^{+6.9}_{-6.3}$	4.83	$1.94 \pm 0.47 \pm 0.52$	5.5σ

perform a binned maximum likelihood fit to the two-dimensional distribution of data in $M(D_s)$ and ΔE , separating the backgrounds from the signal component, which peaks in both. We select events from M_{bc} signal region for this fit. For each of the three D_s^+ decay channels the ΔE range, $-0.1 \text{ GeV} < \Delta E < 0.2 \text{ GeV}$, is divided into 30 bins and the $M(D_s)$ range, $1.5 \text{ GeV}/c^2 < M(D_s) < 2.5 \text{ GeV}/c^2$, into 200 bins. All bins in all D_s^+ submodes are fitted simultaneously to a sum of signal and background shapes. The D_s^+ signal is described by a two-dimensional Gaussian, with widths in both dimensions obtained and fixed using reconstructed signals in the data from $\bar{B}^0 \rightarrow D^+ \pi^- (D^+ \rightarrow K^- \pi^+ \pi^+, K_S \pi^+)$. The signal amplitude is constrained to correspond to the same branching fraction $\mathcal{B}(\bar{B}^0 \rightarrow D_s^+ h^-)$ for all three D_s^+ submodes. The fit also includes an additional two-dimensional Gaussian for $\bar{B}^0 \rightarrow D^+ h^-$ decays.

The background includes three components: combinatorial (linear in $M(D_s)$ and ΔE), $q\bar{q}$ events that peak in $M(D_s)$ and are flat in ΔE , and B decays that peak in ΔE and are flat in $M(D_s)$. The levels of the three components are allowed to vary independently in the three reconstructed D_s^+ modes. The fit results are given in Table I. The statistical significance quoted in Table I is defined as $\sqrt{-2 \ln(\mathcal{L}_0/\mathcal{L}_{max})}$, where \mathcal{L}_{max} and \mathcal{L}_0 denote the maximum likelihood with the fitted signal yield and with the signal yield fixed to zero, respectively. The results of one-dimensional fits to the $M(D_s)$ and ΔE distributions are also shown in Table I for comparison. Figures 2 and 3 show the $M(D_s)$ and ΔE projections for events from the signal region. The sum of the fitted signal plus background is shown by the solid lines while the background shape including the peaking background is indicated by dashed lines. The peaking background is found to be 3.6 ± 0.6 and 3.4 ± 1.3 events for $\bar{B}^0 \rightarrow D_s^+ K^-$ and $B^0 \rightarrow D_s^+ \pi^-$, respectively.

$\bar{B}^0 \rightarrow D_s^{*+} h^-$ final states, where the low energy photon from the $D_s^* \rightarrow D_s \gamma$ decay is missed, can populate the $\bar{B}^0 \rightarrow D_s^+ h^-$ signal region. These would produce a long tail on the negative side of the ΔE distribution. In theoretical models based on factorization, the $B^0 \rightarrow D_s^{*+} \pi^-$ and $B^0 \rightarrow D_s^+ \pi^-$ decay widths are predicted to be approximately equal; there are, however, no corresponding predictions for $\bar{B}^0 \rightarrow D_s^{(*)+} K^-$ decays. To study the sensitivity of the measured branching fraction to a possible $\bar{B}^0 \rightarrow D_s^{*+} h^-$ contribution, we perform a fit with an additional $\bar{B}^0 \rightarrow D_s^{*+} h^-$ component included, where the signal shape is fixed from the MC and the branching fraction is left as a free parameter. The resulting

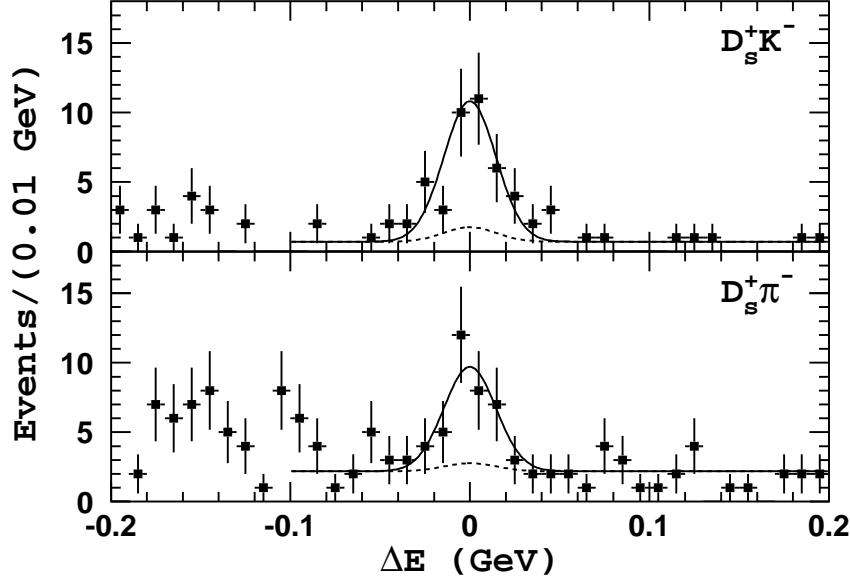


FIG. 3: ΔE spectra for $\bar{B}^0 \rightarrow D_s^+ K^-$ (top) and $B^0 \rightarrow D_s^+ \pi^-$ (bottom) in the B signal region. The points with errors are experimental data and the curves are the results of the simultaneous fit described in the text.

2% difference in the $B^0 \rightarrow D_s^+ \pi^-$ event yield (compared to the results presented in Table I) is added to the systematic uncertainty; the change in the $\bar{B}^0 \rightarrow D_s^+ K^-$ yield is less than 1%. We also check for crossfeed between $\bar{B}^0 \rightarrow D_s^+ K^-$ and $B^0 \rightarrow D_s^+ \pi^-$ due to kaon/pion misidentification. To study this we include the crossfeed contributions in the simultaneous fit, with shapes fixed from the MC and misidentification probabilities obtained from data; the uncertainty due to this effect is found to be negligible ($\lesssim 1\%$).

As a check, we apply the same procedure to $\bar{B}^0 \rightarrow D^+ \pi^-$ and $\bar{B}^0 \rightarrow D^+ K^-$, $D^+ \rightarrow \phi \pi^+$, $\bar{K}^{*0} K^+$, $K_S^0 K^+$, and obtain $\mathcal{B}(\bar{B}^0 \rightarrow D^+ \pi^-) = (2.8 \pm 0.1) \times 10^{-3}$ and $\mathcal{B}(\bar{B}^0 \rightarrow D^+ K^-) = (2.4 \pm 0.4) \times 10^{-4}$ [12], which agree well with the PDG values [11].

The following sources of systematic error are found to be the most significant: tracking efficiency (1-2% per track), charged hadron identification efficiency (1% per particle), K_S^0 reconstruction efficiency (6%), signal-shape parameterization (5%) and MC statistics (2%). The tracking efficiency error is estimated using η decays to $\gamma\gamma$ and $\pi^+\pi^-\pi^0$. The K/π identification uncertainty is determined from $D^{*+} \rightarrow D^0 \pi^+$, $D^0 \rightarrow K^-\pi^+$ decays. We assume equal production of $B^+ B^-$ and $B^0 \bar{B}^0$ pairs but do not include an additional error from this assumption. The uncertainty in the D_s^+ meson branching fractions, which is dominated by the 25% error on $\mathcal{B}(D_s^+ \rightarrow \phi \pi^+)$, is also taken into account. The overall systematic uncertainty is 27%.

In summary, we report the first observation of $B^0 \rightarrow D_s^+ \pi^-$ and an improved measurement of $\bar{B}^0 \rightarrow D_s^+ K^-$. We find $\mathcal{B}(\bar{B}^0 \rightarrow D_s^+ K^-) = (2.93 \pm 0.55 \pm 0.79) \times 10^{-5}$ and $\mathcal{B}(B^0 \rightarrow D_s^+ \pi^-) = (1.94 \pm 0.47 \pm 0.52) \times 10^{-5}$. Since the dominant systematic uncertainty in both measurements is due to the branching fraction for $D_s^+ \rightarrow \phi \pi^+$, $\mathcal{B}_{\phi\pi}$, we also report $\mathcal{B}(\bar{B}^0 \rightarrow D_s^+ K^-) \times \mathcal{B}_{\phi\pi} = (10.5 \pm 2.0 \pm 1.0) \times 10^{-7}$ and $\mathcal{B}(B^0 \rightarrow D_s^+ \pi^-) \times \mathcal{B}_{\phi\pi} = (7.0 \pm 1.7 \pm 0.7) \times 10^{-7}$. These results are consistent with previous results [4, 5] and have better accuracy. They

supersede results from [4].

We thank the KEKB group for the excellent operation of the accelerator, the KEK Cryogenics group for the efficient operation of the solenoid, and the KEK computer group and the National Institute of Informatics for valuable computing and Super-SINET network support. We acknowledge support from the Ministry of Education, Culture, Sports, Science, and Technology of Japan and the Japan Society for the Promotion of Science; the Australian Research Council and the Australian Department of Education, Science and Training; the National Science Foundation of China under contract No. 10175071; the Department of Science and Technology of India; the BK21 program of the Ministry of Education of Korea and the CHEP SRC program of the Korea Science and Engineering Foundation; the Polish State Committee for Scientific Research under contract No. 2P03B 01324; the Ministry of Science and Technology of the Russian Federation; the Ministry of Education, Science and Sport of the Republic of Slovenia; the Swiss National Science Foundation; the National Science Council and the Ministry of Education of Taiwan; and the U.S. Department of Energy.

* on leave from Nova Gorica Polytechnic, Nova Gorica

- [1] M. Kobayashi and T. Maskawa, Prog. Theor. Phys. **49**, 652 (1973).
- [2] C.S. Kim, Y. Kwon, J. Lee, W. Namgung, Phys. Rev. **D 63**, 094506 (2001).
- [3] B. Blok, M. Gronau, J.L. Rosner, Phys. Rev. Lett. **78**, 3999 (1997).
- [4] Belle Collaboration, P. Krokovny *et al.*, Phys. Rev. Lett. **89**, 231804 (2002).
- [5] BaBar Collaboration, B. Aubert *et al.*, Phys. Rev. Lett. **90**, 181803 (2003).
- [6] Belle Collaboration, A. Abashian *et al.*, Nucl. Instr. and Meth. A **479**, 117 (2002).
- [7] S. Kurokawa and E. Kikutani, Nucl. Instr. and Meth. A **499**, 1 (2003).
- [8] Y. Ushiroda (Belle SVD2 Group), Nucl. Instr. and Meth. A **511** 6 (2003).
- [9] R. Brun *et al.*, GEANT 3.21, CERN DD/EE/84-1, 1984.
- [10] CLEO Collaboration, D.M. Asner *et al.*, Phys. Rev. **D 53**, 1039 (1996).
- [11] S. Eidelman *et al.* (Particle Data Group), Phys. Lett. **B 592**, 1 (2004).
- [12] These results should not be considered as a measurements of the corresponding branching fractions since we do not perform analysis of the systematic errors.